Supplementary Information

Nucleation-Controlled Growth of High-Quality $CsPbBr_3$ Single Crystal for Ultrasensitive Weak-Light Photodetector

Xiao Zhao,[ab] Shimao Wang,*[bc] Fuwei Zhuge,[d] Nengwei Zhu,[e] Yanan Song,[bf] Mengyu Fu,[bf] Zanhong Deng,[bc] Xiaodong Fang*[e] and Gang Meng*[bc]

[a] School of Environmental Science and Optoelectronic Technology, University of Science and Technology of China, Hefei 230026, China

[b] Anhui Provincial Key Laboratory of Photonic Devices and Materials, Anhui Institute of Optics and Fine Mechanics, and Key Laboratory of Photovoltaic and Energy Conservation Materials, Hefei Institutes of Physical Science, Chinese Academy of Sciences, Hefei 230031, China

[c] Advanced Laser Technology Laboratory of Anhui Province, Hefei 230037, China

[d] School of Materials Science and Engineering, Huazhong University of Science and Technology, Wuhan 430074, China

[e] College of New Materials and New Energies, Shenzhen Technology University, Shenzhen 518118, China

[f] Science Island Branch of Graduate School, University of Science and Technology of China, Hefei 230026, China

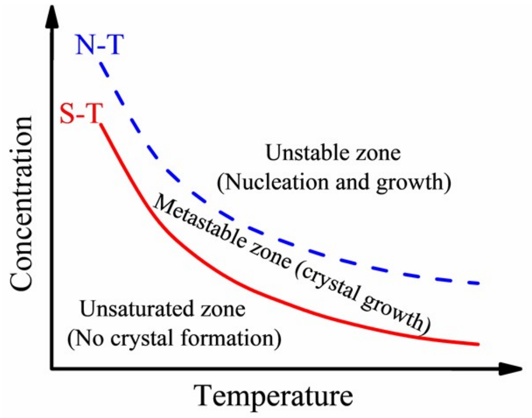

Fig. S1 Schematic diagram of dissolution-nucleation curve of single crystal (SC) grown by solution method with inverse temperature crystallization (ITC) characteristic.

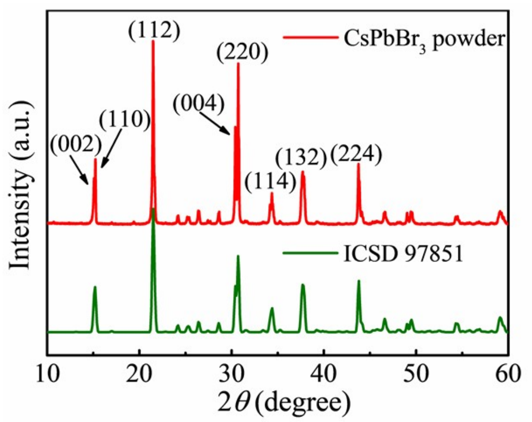

Fig. S2 The powder XRD pattern of the $CsPbBr_3$ SCs grown by the choline bromide (CB) assisted ITC method in comparison with the reported crystal structure of $CsPbBr_3$ (ICSD card #97851).

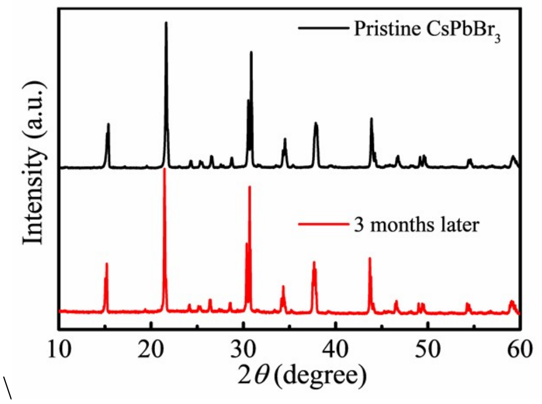

\

Fig. S3 Powder XRD patterns of $CsPbBr_3$ SCs stored for 3 months in air.

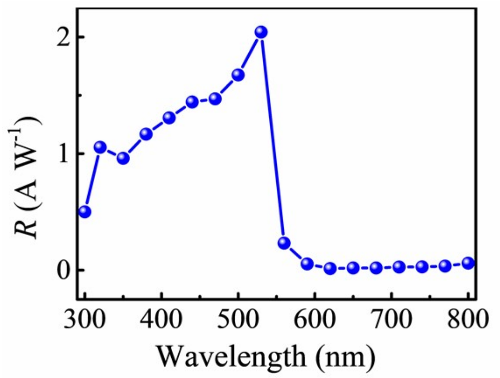

Fig. S4 The variation curve of the wavelength-dependent photoresponsivity of the $CsPbBr_3$ SC (grown from the refined solution) photodetector at the bias of 5 V.

Fig. S5 displays the noise currents for photodetectors based on $CsPbBr_3$ SCs grown from the original solution and the refined solution. It is worth mentioning that the noise current of the photodetector based on $CsPbBr_3$ SCs grown from refined solution is smaller than that grown from original solution. Fig. S6 show the on/off ratio, *R*, and *EQE* dependence on light intensity for photodetectors based on $CsPbBr_3$ SCs grown from the original solution and the refined solution at the bias of 10 V. Under illumination with the same light intensity, on/off ratio, *R*, and *EQE* values for the photodetector based on $CsPbBr_3$ SCs grown from refined solution are higher. In addition, the photodetector based on $CsPbBr_3$ SC grown from the refined solution exhibits faster rise time and decay time (Fig. S7). The higher performance may be attributed to the high crystal quality with fewer trap density, larger carrier mobility, and lower noise current compared with the $CsPbBr_3$ SCs grown from the original solution. Based on the above results, one can conclude that excellent crystal quality and photoelectronic properties can be obtained for the $CsPbBr_3$ SCs grown from refined solution.

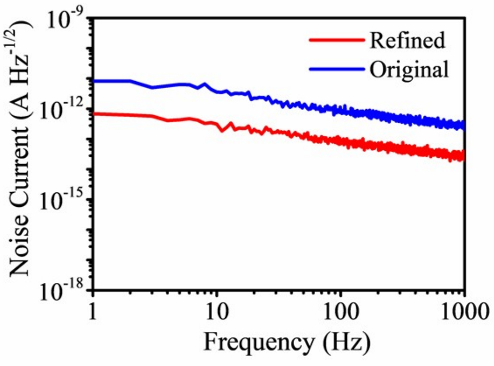

Fig. S5 Noise current versus frequencies of the $CsPbBr_3$ SCs (grown from the original solution and the refined solution) photodetectors from 1 to 1000 Hz at the bias of 5 V.

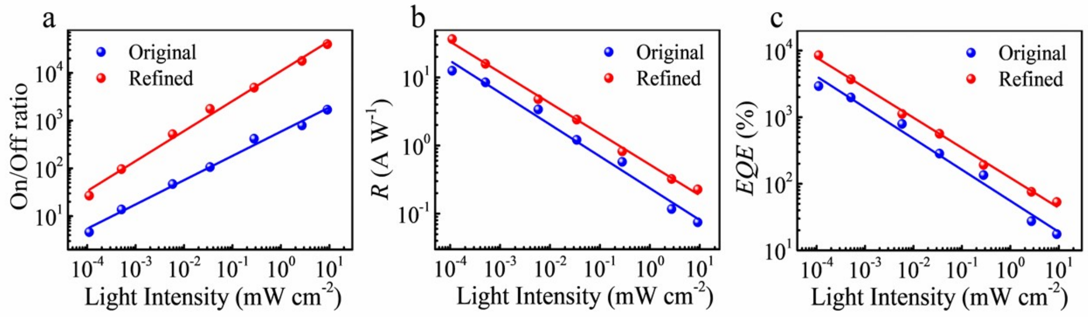

Fig. S6 Comparison of (a) on/off ratio, (b) *R*, and (c) *EQE* dependence on light intensity for photodetectors at the bias of 10 V based on $CsPbBr_3$ SCs grown from original solution and refined solution.

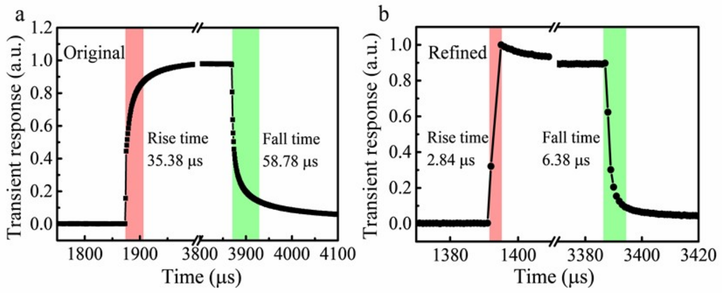

Fig. S7. The local zoom-in of the response times of the photodetectors (a) based on the $CsPbBr_3$ SC grown from the original solution and (b) based on the $CsPbBr_3$ SC grown from the refined solution.

Table S1. Comparisons of trap densities and carrier mobilities of $CsPbBr_3$ SCs

Material	Crystal growth method	Trap density (cm^{-3})	Carrier Mobility ($cm^2\ V^{-1}\ s^{-1}$)	Ref.
$CsPbBr_3$ SC	ITC	4.02×10^9	89.72	This Work
$CsPbBr_3$ SC	ITC	4.2×10^{10}	11±3	1
$CsPbBr_3$ SC film	Space confined method	1.82×10^{10}	1770	2
$CsPbBr_3$ SC	ITC	7.45×10^9	1.06	3
$CsPbBr_3$ SC	Low temperature crystallization in water	1.7×10^{10}	128	4
$CsPbBr_3$ SC film	AVC	5.8×10^{10}	45	5
$CsPbBr_3$ SC film	Space confined method	1.28×10^{10}	2.41	6
$CsPbBr_3$ SC	Bridgman method	1.9×10^9	2060	7
$CsPbBr_3$ SC	Bridgman method	1.08×10^9	1.62	8

Table S2. Performance comparison of $CsPbBr_3$ SCs based photodetector

Method	*R* (light source, intensity, V_{bias})	*EQE*	*D** (Jones)	on/off ratio (intensity, V_{bias})	Ref.
ITC	36.4 A W^{-1} (530 nm, 0.11 μW cm^{-2}, 10 V)	8520%	1.59×10^{13}	3.97×10^4 (9.09 mW cm^{-2}, 2 V)	This work
ITC	6 A W^{-1} (white light, 5 mW cm^{-2}, 10 V)				9

AVC	2.1 A W^{-1} (520 nm, 1 μW)			460 (500 mW cm^{-2}, 6 V)	10
AVC	0.028 A W^{-1} (450 nm, 1 mW cm^{-2}, 5 V)	7%	1.8×10^{11}	100 (5 V)	11
AVC				100	12
ITC	0.028 A W^{-1} (550 nm)	6%	1.7×10^{11}	10^5 (10 mW cm^{-2}, 0 V)	13
Bridgman	2 A W^{-1} (535 nm, 5 V)	460%		10^3 (0.31 mW cm^{-2}, 2 V)	14
Bridgman	5.83 A W^{-1} (532 nm, 1 mW cm^{-2}, 10 V)	1360%	2.5×10^{12}	10^3 (216 μW cm^{-2}, 2 V)	15
space confined	2.5 A W^{-1} (530 nm)	630%	1.4×10^{13}	$>10^3$ (2 V)	16
water-regulated	278 A W^{-1} (520 nm)	66400%	4.36×10^{13}		17
space confined	0.3 A W^{-1} (405 nm, 0.254 mW cm^{-2}, 2.5 V)	95%		3.2×10^3 (1 V)	18

Reference

1 M. I. Saidaminov, M. A. Haque, J. Almutlaq, S. Sarmah, X.-H. Miao, R. Begum, A. A. Zhumekenov, I. Dursun, N. Cho, B. Murali, O. F. Mohammed, T. Wu, O. M. Bakr, *Adv. Optical Mater.*, 2017, **5**, 1600704.

2 Z. Yang, Q. Xu, X. Wang, J. Lu, H. Wang, F. Li, L. Zhang, G. Hu, C. Pan, *Adv. Mater.*, 2018, **30**, 1802110.

3 K. Wang, L. Jing, Q. Yao, J. Zhang, X. Cheng, Y. Yuan, C. Shang, J. Ding, T. Zhou, H. Sun, W. Zhang, H. Li, *J. Phys. Chem. Lett.*, 2021, **12**, 1904–1910.

4 J. Peng, C. Q. Xia, Y. Xu, R. Li, L. Cui, J. K. Clegg, L. M. Herz, M. B. Johnston, Q. Lin, *Nat. Commun.*, 2021, **12**, 1531.

5 Y. Chen, H. Zeng, P. Ma, G. Chen, J. Jian, X. Sun, X. Li, H. Wang, W. Yin, Q. Jia, G. Zou, *Angew. Chem. Int. Ed.*, 2021, **60**, 2629–2636.

6 F. Chen, C. Li, C. Shang, K. Wang, Q. Huang, Q. Zhao, H. Zhu, J. Ding, *Small*, 2022, **18**, 2203565.

7 J. Song, Q. Cui, J. Li, J. Xu, Y. Wang, L. Xu, J. Xue, Y. Dong, T. Tian, H. Sun, H. Zeng, *Adv. Optical Mater.*, 2017, **5**, 1700157.

8 P. Zhang, G. Zhang, L. Liu, D. Ju, L. Zhang, K. Cheng, X. Tao, *J. Phys. Chem. Lett.*, 2018, **9**, 5040–5046.

9 D. N. Dirin, I. Cherniukh, S. Yakunin, Y. Shynkarenko and M. V. Kovalenko, Chem. Mater., 2016, 28, 8470–8474.

10 J.-H. Cha, J. H. Han, W. Yin, C. Park, Y. Park, T. K. Ahn, J. H. Cho and D.-Y. Jung, J. Phys. Chem. Lett., 2017, 8, 565–570.

11 J. Ding, S. Du, Z. Zuo, Y. Zhao, H. Cui and X. Zhan, J. Phys. Chem. C, 2017, 121, 4917–4923.

12 H. Zhang, X. Liu, J. Dong, H. Yu, C. Zhou, B. Zhang, Y. Xu and W. Jie, *Cryst. Growth Des.*, 2017, **17**, 6426−6431.

13 M. I. Saidaminov, M. A. Haque, J. Almutlaq, S. Sarmah, X.-H. Miao, R. Begum, A. A. Zhumekenov, I. Dursun, N. Cho, B. Murali, O. F. Mohammed, T. Wu and O. M. Bakr, *Adv. Opt. Mater.*, 2017, **5**, 1600704.

14 J. Song, Q. Cui, J. Li, J. Xu, Y. Wang, L. Xu, J. Xue, Y. Dong, T. Tian, H. Sun and H. Zeng, *Adv. Opt. Mater.*, 2017, **5**, 1700157.

15 P. Zhang, G. Zhang, L. Liu, D. Ju, L. Zhang, K. Cheng and X. Tao, *J. Phys. Chem. Lett.*, 2018, **9**, 5040–5046.

16 Z. Yang, Q. Xu, X. Wang, J. Lu, H. Wang, F. Li, L. Zhang, G. Hu and C. Pan, *Adv. Mater.*, 2018, **30**, 1802110.

17 X. Wei, H. Liu, Z. Zhang, W. Xu, W. Huang, L.-B. Luo and J. Liu, *Chem Commun*, 2021, **57**, 7798−7801.

18 F. Chen, C. Li, C. Shang, K. Wang, Q. Huang, Q. Zhao, H. Zhu and J. Ding, *Small*, 2022, **45**, 2203565.